# Uncoupling Kap$\beta$2 Substrate Dissociation and Ran Binding

Yuh Min Chook,[‡,§] Astrid Jung,[‡,||] Michael K. Rosen,[⊥,#] and Günter Blobel*[,‡]

*Laboratory of Cell Biology, Howard Hughes Medical Institute, The Rockefeller University, 1230 York Avenue, New York, New York 10021, Universität Regensburg, 93040 Regensburg, Germany, and Howard Hughes Medical Institute, Cellular Biochemistry and Biophysics Program, Memorial Sloan-Kettering Cancer Center, 1275 York Avenue, New York, New York 10021*

*Received December 5, 2001*

ABSTRACT: Karyopherin$\beta$2 (Kap$\beta$2) imports a variety of mRNA binding proteins into the nucleus. Release of import substrates in the nucleus involves formation of a high-affinity Kap$\beta$2−RanGTP complex and concomitant dissociation of import substrates. The crystal structure of the Kap$\beta$2−RanGppNHp complex shows that Ran binds in the Kap$\beta$2 N-terminal arch and substrate most likely binds its C-terminal arch. The structure suggested a mechanism for Ran-mediated substrate dissociation where a long internal acidic loop in Kap$\beta$2 transmits structural information between the GTPase and substrate sites, leading to displacement of substrate by the loop when Ran is bound. To study the molecular mechanism of substrate dissociation, we have cleaved the acidic loop of Kap$\beta$2 proteolytically (cl-Kap$\beta$2) and also constructed a mutant of Kap$\beta$2 with a truncated loop (TL-Kap$\beta$2). Both modified Kap$\beta$2s are unable to undergo Ran-mediated substrate dissociation. We have also mapped the boundaries of the Kap$\beta$2 binding site of substrate mRNA binding protein A1 using a widely applicable method employing NMR spectroscopy. This has allowed design of reagents to quantitate the affinities of the Kap$\beta$2 proteins for Ran and substrate. cl-Kap$\beta$2, TL-Kap$\beta$2, and native Kap$\beta$2 have comparable affinities for both RanGppNHp and import substrates, indicating that perturbation of the loop has not altered the strength of binary Kap$\beta$2−Ran or Kap$\beta$2−substrate interactions. The TL-Kap$\beta$2 mutant also binds RanGppNHp and substrate simultaneously to form a ternary complex, indicating that in addition to the loss of coupling between Ran binding and substrate dissociation, the two ligand sites on Kap$\beta$2 are spatially distinct. The uncoupling of Ran binding and substrate dissociation in the TL-Kap$\beta$2 mutant is further evident in significant loss of Ran-mediated nuclear uptake of fluorescent substrate in digitonin-permeabilized HeLa cells. These results support our previously proposed GTPase-mediated Kap$\beta$2−substrate dissociation mechanism where the acidic loop of Kap$\beta$2 physically couples distinct Ran and substrate binding sites.

Kap$\beta$2[1] mediates nuclear import of many mRNA binding proteins such as A1, A2, F, and TAP (*1*−*4*). Kap$\beta$2 is a member of the karyopherin $\beta$ (Kap$\beta$) family of proteins, all of which share similar molecular masses (90−150 kDa) and contain multiple HEAT repeats [reviewed in (*5*)]. Of the 14 Kap$\beta$s in yeast and more than 20 in mammalian cells, most have identified functions in nuclear import (import Kaps are also known as Importins), export (export Kaps are also known as Exportins), or bidirectional nuclear transport (*6*). Import Kap$\beta$s interact with both the nuclear localization signal (NLS) of import substrate and the nuclear pore complex (NPC), thus targeting substrate to the NPC. Kap$\beta$2 interacts directly with a 39 amino acid sequence at the C-terminus of mRNA binding protein A1 termed the M9-NLS (*1*, *2*). mRNA binding protein A2 also contains an M9-NLS with strong sequence similarity to that in A1. However, the NLS for mRNA binding protein F remains unidentified, and the NLS for TAP shares no sequence homology with the M9-NLS in A1 (*2*−*4*). It appears that although all known import substrates for Kap$\beta$2 share common functions in mRNA processing and export, their NLSs and thus their modes of interaction with the karyopherin may be diverse.

Substrate−Kap$\beta$ interactions are regulated by the Ran GTPase [reviewed in (*5*)]. Binding of import Kap$\beta$s to import substrates and RanGTP is mutually exclusive, leading to a model where high-affinity binding of the GTPase to Kap$\beta$ results in substrate dissociation in the nucleus. Asymmetric intracellular localization of Ran regulators, RanGAP (catalyzes Ran nucleotide hydrolysis) to the cytoplasm and the cytoplasmic fibers of the NPC and RanGEF (catalyzes Ran nucleotide exchange) to chromatin and the NPC nuclear basket, likely results in an asymmetric pool of nuclear RanGTP. Such distribution of RanGDP in the cytoplasm and

* To whom correspondence should be addressed at the Laboratory of Cell Biology, Howard Hughes Medical Institute, The Rockefeller University, 1230 York Ave., New York, NY 10021. Tel: (212) 327-8096. Fax: (212) 327-7880. E-mail: blobel@rockvax.rockefeller.edu.

‡ The Rockefeller University.

§ Present address: Department of Pharmacology, University of Texas Southwestern Medical Center, Dallas, TX 75390.

|| Universität Regensburg.

⊥ Memorial Sloan-Kettering Cancer Center.

# Present address: Department of Biochemistry, University of Texas Southwestern Medical Center, Dallas, TX 75390.

[1] Abbreviations: Kap, karyopherin; NLS, nuclear localization signal; NPC, nuclear pore complex; GFP, green fluorescent protein; MBP, maltose binding protein; GST, glutathione *S*-transferase; SPR, surface plasmon resonance; GAP, GTPase activating protein; GEF, guanine nucleotide exchange factor; TL, truncated loop; cl, cleaved; HSQC, heteronuclear single quantum coherence; TAP, Tip associated protein.

10.1021/bi012122p CCC: $22.00 
Published on Web 05/10/2002

RanGTP in the nucleus allows GTPase-mediated Kap$\beta$−substrate dissociation to occur in the nucleus. GTPase-mediated substrate dissociation and other means of substrate release such as nuclear target-aided substrate dissociation and NPC-pseudosubstrate sequence-mediated substrate dissociation, all contribute to the final import step in the nucleus (*7*−*9*).

The crystal structure of full-length Kap$\beta$2 bound to RanGppNHp provides a picture of one of the final steps of nuclear import (*10*). Kap$\beta$2 contains 20 HEAT repeats that stack to form an extended superhelical spiral, which is further organized into 2 approximately perpendicular, contiguous arches (Figure 1a). A striking departure from the helical structure of Kap$\beta$2 is the 62-residue acidic loop inserted between the helices of HEAT repeat 8. RanGppNHp interacts with the concave surface of the N-terminal arch of Kap$\beta$2 through two contact areas: the first involves the first four HEAT repeats, which interact with the switch I and switch II regions of Ran; the second involves the central HEAT repeats 7, 8 and the acidic loop, which interact with the 'basic patch' $\alpha$4-$\alpha$5 region of Ran. The structure of the Kap$\beta$2−Ran complex, in combination with previous biochemical studies using Kap$\beta$2 deletion mutants, also allowed assignment of the substrate binding site of Kap$\beta$2 to the concave surface of its C-terminal arch (*2*, *10*, *11*). The Kap$\beta$2−Ran structure strongly suggests an allosteric mechanism for GTPase-mediated substrate dissociation. The proximal portion of the 62-residue acidic loop of Kap$\beta$2 interacts extensively with Ran while its distal portion resides in the C-terminal arch where substrate is predicted to bind. We proposed that the acidic loop of Kap$\beta$2 transmits structural information between the GTPase and substrate binding sites and displaces substrate in the C-terminal arch upon Ran binding (*10*).

In this paper, we present biochemical and biophysical evidence to support the allosteric mechanism for GTPase-mediated substrate dissociation where the Kap$\beta$2 acidic loop transmits allosteric effect from Ran to the substrate site. To study the molecular mechanism of substrate dissociation, we have disrupted the polypeptide chain of the Kap$\beta$2 acidic loop by specific proteolytic cleavage (cl-Kap$\beta$2) and also constructed a mutant of Kap$\beta$2 with truncated acidic loop (TL-Kap$\beta$2). We also mapped the extensive binding site on substrate A1 for Kap$\beta$2 using a widely applicable method employing NMR spectroscopy, extending the minimal M9 sequence (*2*, *12*) to a 66-residue fragment (residues 254−320). This information has allowed us to generate reagents to quantitate affinities of Kap$\beta$2−substrate interactions. Dissociation constants, $K_D$s, measured in fluorescence titration experiments show that although cl-Kap$\beta$2, TL-Kap$\beta$2, and native Kap$\beta$2 have comparable high affinities for both RanGppNHp and import substrates A1 and TAP, RanGTP is unable to dissociate substrate from the mutant proteins. The uncoupling of RanGTP binding and substrate dissociation in the TL-Kap$\beta$2 mutant is further evident in significant loss of Ran-mediated nuclear import in digitonin-permeabilized HeLa cells. TL-Kap$\beta$2 also binds RanGppNHp and substrate simultaneously to form a Ran−TL-Kap$\beta$2−substrate ternary complex, suggesting that Ran and substrate binding sites on Kap$\beta$2 are spatially distinct and that coupling between those sites in the native protein is mediated by the acidic loop. These studies strongly support our previously proposed GTPase-mediated Kap$\beta$2−substrate dissociation mechanism (*10*). The 62-residue acidic loop of Kap$\beta$2 physically couples distinct Ran and substrate binding sites. When RanGTP binds to the N-terminal arch of Kap$\beta$2, a conformational change is transmitted through the acidic loop to the remote substrate binding site in the Kap$\beta$2 C-terminal arch.

## MATERIALS AND METHODS

*Protein Expression and Purification.* Kap$\beta$2 was expressed in a modified pGEX4T3 (Pharmacia) vector with a Tev protease cleavage site, using *E. coli* BL21-DE3. The protein was purified as described in (*10*). cl-Kap$\beta$2 is generated by cleaving purified Kap$\beta$2 to completion with thrombin (Sigma) and stopping the cleavage reaction with hirudin (Sigma) followed by further purification on a Superdex 200 column (Pharmacia). Expression construct for TL-Kap$\beta$2 was generated by replacing a gene fragment coding for the acidic loop (restriction digest fragment *Nsi*I−*Dra*III) with a PCR product encoding a truncated loop (Figure 1c). TL-Kap$\beta$2 protein was purified as described for Kap$\beta$2.

Ran was expressed in a pET9c (Novagen) vector using *E. coli* BL21-DE3. Purification of the protein and loading with nucleotide were as described previously (*10*). Fragments M3 of substrate A1 were cloned into expression vectors pGEX4T3 (Pharmacia) and pMalc2 (NEB) to produce GST and MBP fusion proteins. A shorter M3 fragment with a single site mutation, M3a-F247C (Figure 2), was cloned into pMalc2 to produce MBP-M3aY247C. Substrates were expressed using *E. coli* BL21-DE3. GST-M3 was purified using glutathione−Sepharose (Pharmacia) affinity column. MBP fusion proteins were purified with two successive anion exchange chromatography steps at pH 7.3 and pH 8.0, then by gel filtration. TAP-NLS [TAP residues 61−102; (*4*)] was amplified from a human fetal brain cDNA library (Clontech) and cloned into the modified pGEX4T3 vector. GST-TAP-NLS was purified by affinity chromatography, cleaved with Tev protease, and further purified by gel filtration.

$^{15}$N-GST-M3 was expressed using *E. coli* BL21-DE3 transformed with pGEX4T3-(tev)M3 and grown at 37 °C in $^{15}NH_4Cl$ M9 minimal media. $^{15}$N-GST-M3 was partially purified using glutathione−Sepharose. An excess of $^{15}$N-GST-M3 was added to Kap$\beta$2, cleaved with Tev protease, and then further purified by gel filtration (buffer contains 50 mM sodium phosphate, 100 mM NaCl, 1 mM EDTA, 5 mM DTT, 5% glycerol, pH 6.8).

Additional proteins were purified for import and export assays. MPB-M3-GFP was expressed in a pMalc2 vector using *E. coli* BL21-DE3. Purification was as described above for other MBP-M3 proteins. Kap$\beta$1 was expressed in a pGEX6P1 vector (Pharmacia), and purified using a protocol similar to that for Kap$\beta$2, except Precission protease (Pharmacia) is used instead of Tev protease. CAS was expressed in a modified pGEX4T3 vector, using *E. coli* BL21-DE3. Purification was as described for Kap$\beta$2 (*10*). Mouse Kap$\alpha$ was expressed in a pET21a (Novagen) vector, and purified by affinity chromatography using Talon beads (Novagen) followed by anion exchange chromatography and gel filtration. RanBP1 for import/export assays was expressed in a pET11d (Novagen) vector and purified by anion exchange chromatography and gel filtration. $His_6$-p10/NTF2 was

purified by affinity chromatography using Talon beads followed by gel filtration. All purified proteins were stored at 4 °C in TB buffer (20 mM Hepes, pH 7.3, 110 mM potassium acetate, 1 mM EGTA, 2 mM magnesium acetate, 2 mM DTT, and 20% glycerol).

*Dissociation and Binding Experiments*. Binding of substrate fragment M3 to Kap$\beta$2 proteins was monitored qualitatively in a binding assay where approximately 17 $\mu$g of Kap$\beta$2 protein was added to 10 $\mu$L of glutathione−Sepharose beads loaded with GST-M3 (~3 $\mu$g of GST-M3/10 $\mu$L of beads). The beads were then washed 3 successive times, each time with 0.5 mL of TB buffer. This is followed by a second incubation with either buffer, RanGDP, or RanGppNHp (4.8 $\mu$g of Ran/10 $\mu$L of beads). After three successive 0.5 mL washes with TB buffer, the beads were subjected to SDS−PAGE. All experiments were done at 4 °C. Binding of RanGppNHp to Kap$\beta$2 proteins was monitored qualitatively by gel filtration; 75 $\mu$g of Kap$\beta$2 protein was added to 52.8 $\mu$g of RanGppNHp and loaded onto a Superdex 200 column. Elution volumes of all protein peaks were recorded, and eluted fractions were collected and visualized with SDS−PAGE. Samples of free TL-Kap$\beta$2, TL-Kap$\beta$2 complexed with MBP-M3, TL-Kap$\beta$2 complexed with RanGppNHp, and TL-Kap$\beta$2 complexed with both RanGppNHp and MBP-M3 were subjected to similar gel filtration experiments.

*NMR Experiments.* $^{1}$H/$^{15}$N HSQC spectra (*13*) were recorded on a 600 MHz Varian Inova instrument on a 180 $\mu$M sample of a 1:1 complex of $^{15}$N-labeled M3 peptide and unlabeled Kap$\beta$2 in buffer containing 50 mM sodium phosphate, pH 6.8, 100 mM sodium chloride, 1 mM EDTA, 2 mM dithiothreitol, and 5% glycerol. Spectra were recorded at 25 °C with $^{1}$H and $^{15}$N sweep widths of 9000 and 2000 Hz, respectively, 576 and 128 complex points in the $^{1}$H and $^{15}$N dimensions, respectively, and 256 transients per indirect increment.

*Fluorescent Labeling of Proteins.* All proteins to be labeled were exchanged into TB buffer free of DTT. Labeling of MBP-M3-F247C with AlexaFluor 350 C2 maleimide and mouse Kap$\alpha$ with Texas red C2 maleimide was performed by incubating the proteins with 5-fold molar excess of fluorophores at 4 °C for 2 and 0.5 h, respectively. Free fluorophore was removed using a HiTrap desalting column (Pharmacia), and AlexaFluor 350-labeled MBP-M3-F247C (MBP-AlexaFluor350-M3) was quantitated by its absorbance at 350 nm. RanGDP was incubated with >5-fold molar equivalent of the *N*-methylanthraniloyl (mant) derivative of GppNHp (JenaBiosciences), in the presence of alkaline phosphatase−agarose, for 24 h at 4 °C. Ran(mant)GppNHp was purified by gel filtration on Superdex 75, and its concentration was quantitated by the absorbance at 350 nm.

*Fluorescence Titration.* Experiments to determine the binding constants of RanGppNHp for Kap$\beta$2 proteins were performed on a Fluoromax2-spectrofluorometer (Spex Inc.), at 15 °C, using 10 nM Ran(mant)GppNHp in TB buffer. A decrease in the mant fluorescence was monitored at 466 nm ($\lambda_{excitation}$ = 350 nm) as Kap$\beta$2 proteins were titrated. The data were fitted through nonlinear regression to a quadratic equation describing a simple bimolecular association process to obtain values for $K_D$. At least three independent titrations were performed for each interaction. Affinities of substrate fragment M3 for Kap$\beta$2 proteins were determined in a similar manner; 15 nM MPB-AF350-M3 was titrated with Kap$\beta$2 proteins, and the increase in fluorescence at 445 nm ($\lambda_{excitation}$ = 345 nm) was monitored.

*SPR Analysis*. Kap$\beta$2/TAP-NLS and TL-Kap$\beta$2/TAP-NLS association and dissociation were studied by surface plasmon resonance (SPR) using a BIAcore 2000 instrument (Pharmacia BIOsensors) which allows monitoring of real time binding. All measurements were carried out at a flow rate of 5 $\mu$L/min and 25 °C, using running buffer 20 mM Na-HEPES, pH 7.4, 150 mM NaCl, 5 mM $MgCl_2$, and surfactant, 0.005% polyoxyethylenesorbitan. TAP-NLS was immobilized onto a CM5-sensorchip following the standard coupling protocol of the manufacturer. Direct amide coupling to the surface could be used without partial inactivation of the ligand due to the absence of lysine residues and was highly preferred to a sandwich assay. The latter seemed to generate a complicated system of unspecific interactions; 25−35 $\mu$g of TAP-NLS in 50 mM HEPES, 0.5 mM NaCl, pH 7.5, was immobilized to the activated surface, charging the chip to approximately 400 resonance units, followed by inactivation of uncoupled functional sites with ethanolamine. Background surfaces were generated under identical conditions, but without NLS. The best surface regeneration was accomplished with 10 mM glycine, pH 2.0, followed by 0.05% SDS. Binding of Kap$\beta$2 and TL-Kap$\beta$2 to TAP-NLS was analyzed in a concentration-dependent mode using the BIAlogue 2.1 evaluation software. Background response signals were subtracted from respective signals obtained from the specific binding reactions for all concentrations of Kap$\beta$2 and TL-Kap$\beta$2. The resulting curves were fitted to a Langmuir binding model after correction for mass-transfer-limitation effects. $\chi_2$ values below 10 indicate good fit to the selected model.

*Import/Export Assays.* HeLa cells were grown to ~50% confluency on coverslips, washed in cold TB buffer, and permeabilized with 35 $\mu$g/mL digitonin on ice for 5 min. Permeabilized cells were incubated with import reaction mixture (containing various combinations of karyopherins, fluorescent transport substrate, Ran, GTP, and other transport factors such as RanBP1 and p10/NTF2) for 20 min at 20 °C followed by washing and fixing.

For export assays, HeLa cells on coverslips were permeabilized as described for import assays and incubated with import reaction mixture containing fluorescent export substrate, its import karyopherins, and a Ran mix (Ran, RanBP1, p10/NTF2, and GTP) for 20 min at 20 °C. Cells were washed and then incubated with export reaction mixture (containing karyopherins, Ran, GTP, RanBP1, and p10/NTF2) for 20 min at 20 °C, washed, and fixed.

## RESULTS

*The Acidic Loop of Kap$\beta$2 Is Disrupted by Specific Proteolysis or Truncation Mutagenesis.* Kap$\beta$2 is an exclusively helical protein, with a 62-residue internal loop that is its only significant deviation from helical structure (*10*). A striking characteristic of this loop is the presence of two stretches of acidic residues, $^{321}$DVEEDE$^{326}$ and $^{350}$DEDGIEEEDDDDDEIDDDD$^{368}$ (Figure 1a). A much shorter 11-residue acidic loop is also present in Kap$\beta$1, and has been observed in the structures of a Kap$\beta$1−Kap$\alpha_{11-54}$ complex and a Kap$\beta1_{1-462}$−RanGppNHp complex (*14*, *15*). A similar

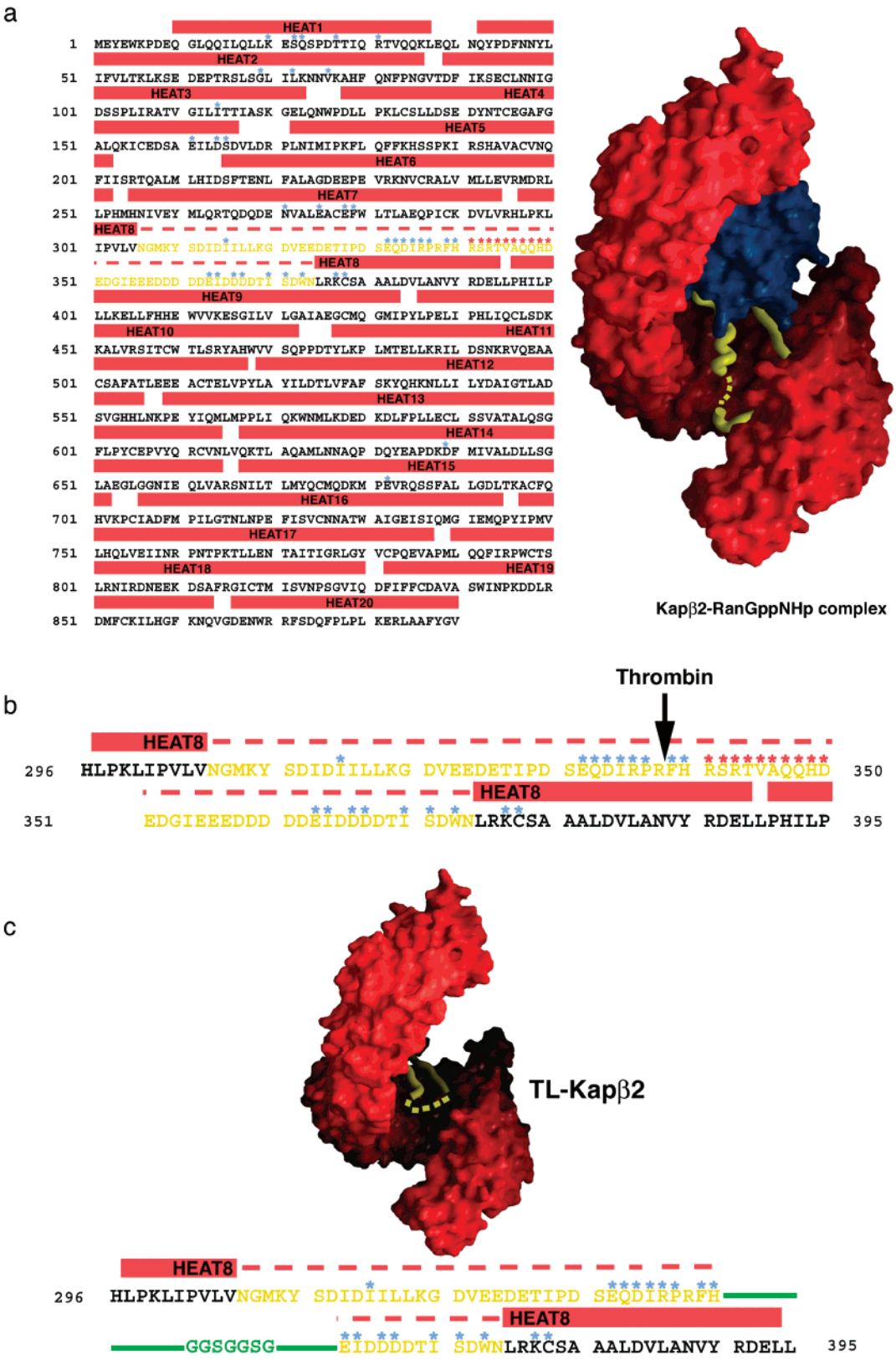


FIGURE 1: Structure of Kap$\beta$2−RanGppNHp complex and modifications to produce cl-Kap$\beta$2 and TL-Kap$\beta$2. (a) Primary and secondary structures of Kap$\beta$2 as well as the crystal structure of Kap$\beta$2−RanGppNHp represented with a GRASP surface (*30*). Kap$\beta$2 is in red, the Kap$\beta$2 acidic loop is in yellow (dashed yellow line represents disordered residues in the loop), and RanGppNHp is in blue. Kap$\beta$2 HEAT repeats are represented by a red strip above the Kap$\beta$2 sequence. Residues in the acidic loop are in yellow, and Kap$\beta$2 residues that interact with RanGppNHp are marked with blue asterisks while acidic loop residues that interact with the C-terminal arch are labeled with red asterisks. (b) Amino acid sequence of the acidic loop is shown with the thrombin cleavage site. (c) A model of TL-Kap$\beta$2, with residues 341−362 removed and replaced with GGSGGSG linker.

acidic loop is also predicted in Kap$\beta$3 (*16*). In the structure of the Kap$\beta$2−RanGppNHp complex, Kap$\beta$2 HEAT repeats are arranged into a spiral of two orthogonal arches (*10*). The acidic loop emanates from the N-terminal arch. Some of the

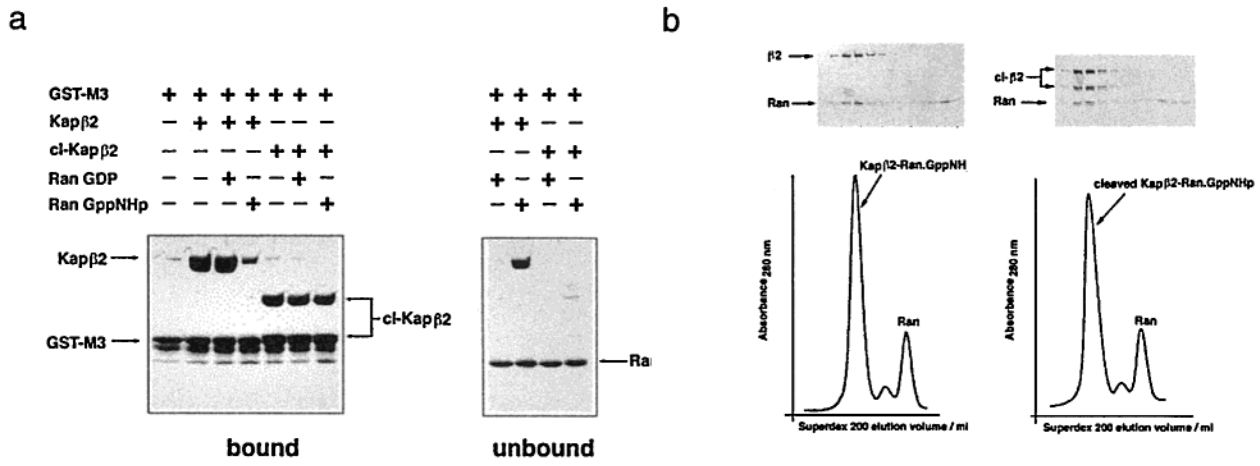


FIGURE 2: cl-Kap$\beta$2 binds Ran and substrate M3, but substrate is not dissociated in the presence of RanGppNHp. (a) GST-M3 is immobilized on glutathione−Sepharose and incubated with 17 $\mu$g of either Kap$\beta$2 or cl-Kap$\beta$2. After washing, dissociation was done with an excess of either RanGDP or RanGppNHp (4.8 $\mu$g). Bound and unbound proteins are visualized by SDS−PAGE and Coomassie blue staining. (b) A mixture of 75 $\mu$g of Kap$\beta$2 or 105 $\mu$g of cl-Kap$\beta$2 and 52.8 $\mu$g of RanGppNHp was loaded onto a Superdex 200 column. Elution profiles of both complexes are shown. 25 $\mu$L of each eluted fraction (0.5 mL/fraction) was visualized with SDS−PAGE with Coomassie Blue staining.

loop residues interact extensively with Ran (blue asterisks in Figure 1a), and other residues interact with the concave surface of the C-terminal arch where substrates are proposed to bind [red asterisks in Figure 1a (*2*, *10*, *11*)]. The distinct location of the Kap$\beta$2 ligand binding sites and the structure of the acidic loop in the GTPase complex suggest an allosteric mechanism for GTPase-mediated substrate dissociation with a crucial role for the acidic loop in transmission of the allosteric effect.

We sought to disrupt or modify the Kap$\beta$2 acidic loop to investigate its role in Ran-mediated substrate dissociation. Thrombin cleaves the 101 kDa Kap$\beta$2 into two fragments of approximately 40 and 60 kDa (cl-Kap$\beta$2; Figures 1b and 2a). N-terminal sequencing of the fragments indicates cleavage at a major site between residues 338 and 339 (Figure 1b), and at a minor site (<5% of total cleavage) between residues 343 and 344. Since most of the acidic loop does not contact the main body of the karyopherin, the three-dimensional structure of cl-Kap$\beta$2 should be similar to intact Kap$\beta$2 with the exception of the severed loop (*10*). This prediction is supported by size exclusion chromatography of cl-Kap$\beta$2 where both fragments coelute with a profile identical to intact Kap$\beta$2 (Figure 1 of the Supporting Information).

Binding sites on the acidic loop for Ran and the C-terminal arch of Kap$\beta$2 are nonoverlapping (Figure 1b) (*10*). We constructed a Kap$\beta$2 mutant where residues in the loop that interact with and reside in the C-terminal arch are removed but residues that contact Ran are maintained. Residues 341−362 were removed and replaced with a 7-residue flexible GGSGGSG linker, generating mutant protein TL-Kap$\beta$2 (Figure 1c). The gel filtration elution profile of TL-Kap$\beta$2 is similar to that of intact Kap$\beta$2, indicating that the gross dimensions of the mutant and wild-type proteins are similar. Furthermore, the circular dichroism spectra of all three proteins, Kap$\beta$2, cl-Kap$\beta$2, and TL-Kap$\beta$2, are similar (Figure 2 of the Supporting Information).

Proteolytic cleavage of the acidic loop abolishes Ran-mediated substrate dissociation. The M3 fragment of mRNA binding protein A1 (residues 235−320) (*12*) was expressed as an N-terminal GST fusion protein and immobilized on glutathione−Sepharose. In a qualitative binding assay where immobilized GST-M3 was incubated with Kap$\beta$2 or cl-Kap$\beta$2, both cleaved and intact Kap$\beta$2s bind substrate equally well (Figure 2a, lanes 2 and 5). Kap$\beta$2−Ran interactions were studied by gel filtration analyses of mixtures of RanGppNHp with either cl-Kap$\beta$2 or intact Kap$\beta$2. The proteins show similar size exclusion chromatography profiles (Figure 2b), indicating similar high-affinity binding to RanGppNHp.

Kap$\beta$2 can be specifically dissociated from its substrate by RanGppNHp, but not RanGDP (Figure 2a, lanes 3 and 4). In contrast, the immobilized cl-Kap$\beta$2−M3 complex could not be dissociated by RanGppNHp (Figure 2a, lanes 6 and 7). These results indicate that RanGppNHp binding is coupled to substrate dissociation in intact Kap$\beta$2, but disruption of the polypeptide chain of the acidic loop in cl-Kap$\beta$2 has uncoupled Ran binding from substrate dissociation. Thus, the intact acidic loop is necessary to mediate interactions between the Ran and substrate binding sites of Kap$\beta$2.

*Kap$\beta$2 Mutant with a Truncated Acidic Loop Forms a Ternary Complex with Ran and Substrate.* A qualitative binding assay using M3 immobilized on glutathione−Sepharose shows that TL-Kap$\beta$2 binds substrate M3 with similar high affinity as intact Kap$\beta$2 (Figure 3a, lanes 1 and 4). Gel filtration chromatography also shows that TL-Kap$\beta$2 binds RanGppNHp with high affinity (Figure 3b). However, in comparison with intact Kap$\beta$2, TL-Kap$\beta$2 is not significantly displaced from immobilized M3 by RanGppNHp (Figure 3a, compare lanes 3 and 6). Furthermore, RanGppNHp binds to the immobilized TL-Kap$\beta$2−M3 complex, indicating formation of a RanGppNHp−TL-Kap$\beta$2−M3 ternary complex. This ternary complex is even more evident in gel filtration experiments where TL-Kap$\beta$2 is incubated with excess RanGppNHp and MBP-M3. A large molecular mass complex containing stoichiometric amounts of all three proteins elutes earlier than the binary TL-Kap$\beta$2−Ran and TL-Kap$\beta$2−MBP-M3 complexes (Figure 3b,c). Based on calibration of the Superdex 200 column using gel filtration

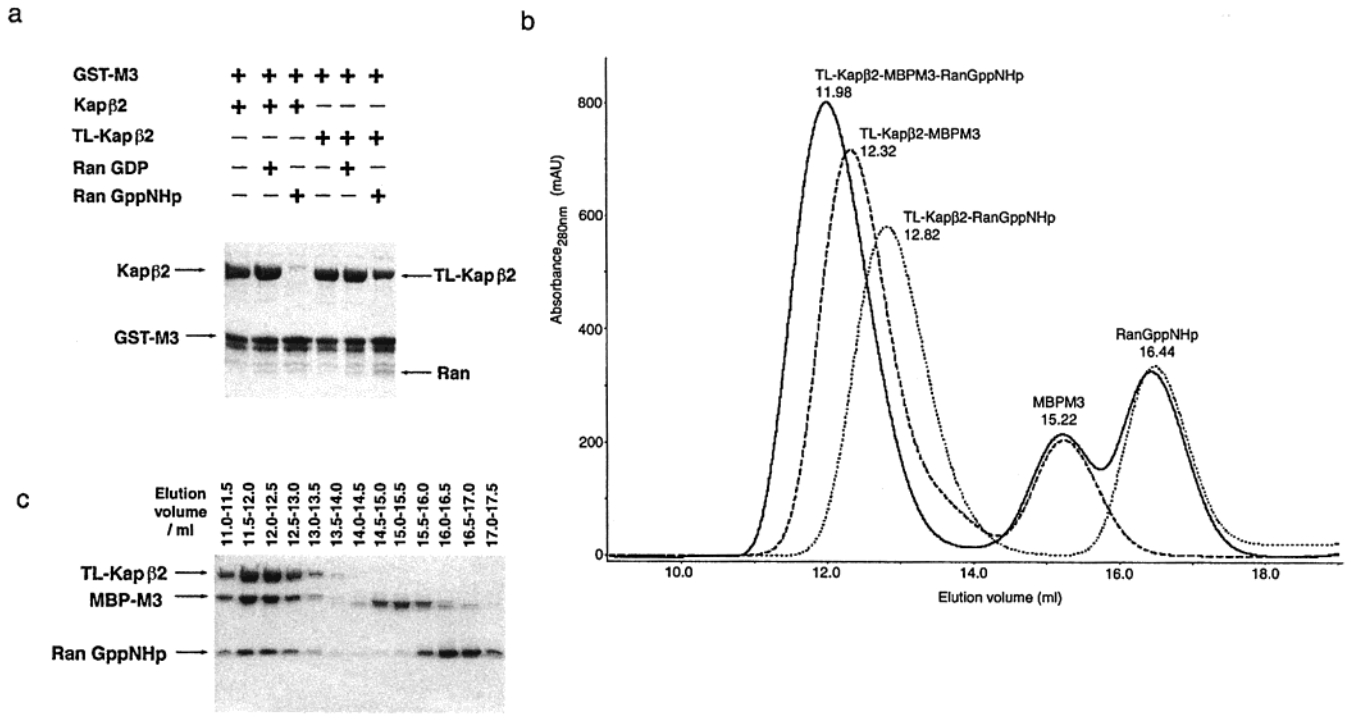


FIGURE 3: Significant decrease of substrate from TL-Kap$\beta$2 in the presence of RanGppNHp, and TL-Kap$\beta$2 binds Ran and substrate simultaneously to form a ternary complex. (a) GST-M3 is immobilized on glutathione−Sepharose and incubated with 17 $\mu$g of either Kap$\beta$2 or TL-Kap$\beta$2. After washing, dissociation was done with an excess of either RanGDP or RanGppNHp (4.8 $\mu$g), and bound proteins were visualized by SDS−PAGE and Coomassie blue staining. (b) Mixtures of 720 $\mu$g of TL-Kap$\beta$2 and either 570 $\mu$g of MBP-M3 or 750 $\mu$g of RanGppNHp were loaded onto a Superdex 200 column where TL-Kap$\beta$2−MBP-M3 or TL-Kap$\beta$2−RanGppNHp binary complexes were separated from excess substrate and Ran. A mixture of 720 $\mu$g of TL-Kap$\beta$2, 570 $\mu$g of MBP-M3, and 750 $\mu$g of RanGppNHp was also subjected to gel filtration. Elution profiles of the three gel filration experiments were overlayed. (c) 10 $\mu$L of each eluted fraction (0.5 mL/fraction) from gel filtration experiment in (b) of 720 $\mu$g of TL-Kap$\beta$2, 570 $\mu$g of MBP-M3, and 750 $\mu$g of RanGppNHp was visualized with SDS−PAGE/Coomassie Blue staining.

molecular mass standards, the RanGppNHp−TL-Kap$\beta$2−M3 ternary complex elutes with similar hydrodynamic behavior as a 180 kDa protein whereas binary TL-Kap$\beta$2−Ran elutes similar to a 124 kDa molecule and binary TL-Kap$\beta$2−MBP-M3 behaves like a 150 kDa molecule, all in close agreement with the actual molecular masses of the respective complexes.

These results indicate that removal of acidic loop residues that interact with the putative Kap$\beta$2 substrate site has significantly disabled Ran-mediated substrate dissociation. Thus, the acidic loop is indeed crucial for transmission of the signal from Ran to the substrate binding site. Furthermore, truncation of the acidic loop allows both Ran and substrate to bind the Kap$\beta$2 mutant simultaneously, suggesting that the two ligand binding sites are spatially distinct.

*Establishing Boundaries of the Kap$\beta$2 Binding Site on M3 by NMR Spectroscopy.* Previous studies have demonstrated that the minimal NLS for Kap$\beta$2, M9-NLS (A1 residues 268−305), lies within the M3 peptide (A1 residues 228−320) (*2*, *12*). To precisely define the boundaries of the minimal interaction region, we analyzed a complex of $^{15}$N-labeled M3 peptide bound to Kap$\beta$2 using NMR spectroscopy. A $^{1}$H/$^{15}$N HSQC spectrum of the complex is shown in Figure 4a. In spectra of this type, only signals corresponding to $^{15}$N-labeled components can be observed. Thus, the data represent exclusively the labeled M3 peptide. Ideally, the backbone amide (NH) of each residue in the peptide should give rise to a single signal in the two-dimensional plane. Each side chain amide ($NH_2$) of glutamine and asparagine residues should give rise to two signals, with distinct proton chemical shifts that share a common $^{15}$N chemical shift. However, signal intensity in NMR spectra is directly related to the mobility/tumbling rate in solution (*17*). Thus, portions of M3 that are immobilized on the surface of Kap$\beta$2, and tumble at the slow rate of a 110 kDa system, will have very weak signals. In contrast, regions of the peptide that are not part of the binding epitope are likely to remain highly mobile in the complex, and are expected to have more intense signals. In $^{1}$H/$^{15}$N HSQC spectra, glycine backbone amides typically show distinctive signals, with unique $^{15}$N chemical shifts in the 104−112 ppm range. Side chain amides are also distinct, with pairs of signals having $^{1}$H chemical shifts between 6.5 and 8.5 ppm and $^{15}$N chemical shifts between 110 and 115 ppm.

The $^{1}$H/$^{15}$N HSQC spectrum in Figure 4a, plotted to display only very intense signals, contains approximately 11 peaks in the region typical of glycine (area of interest is enlarged in inset), and 8 peaks corresponding to other residue types. In addition, 4 pairs of intense side chain amide signals can be observed. Assuming that the binding epitope is continuous, we expect that the observed signals should represent glycine and asparagine/glutamine residues at the ends of M3. A 28-residue segment containing 4 asparagine/glutamine residues at the N-terminus would contain 11 glycine residues (excluding the N-terminal residue, which has an amine rather than an amide), which is in coincidence with the NMR data. In contrast, C-terminal asparagine/glutamine residues are only found in the segment containing the M9 sequence, which has been shown to be necessary in entirety for Kap$\beta$2 binding. Thus, it appears very likely that

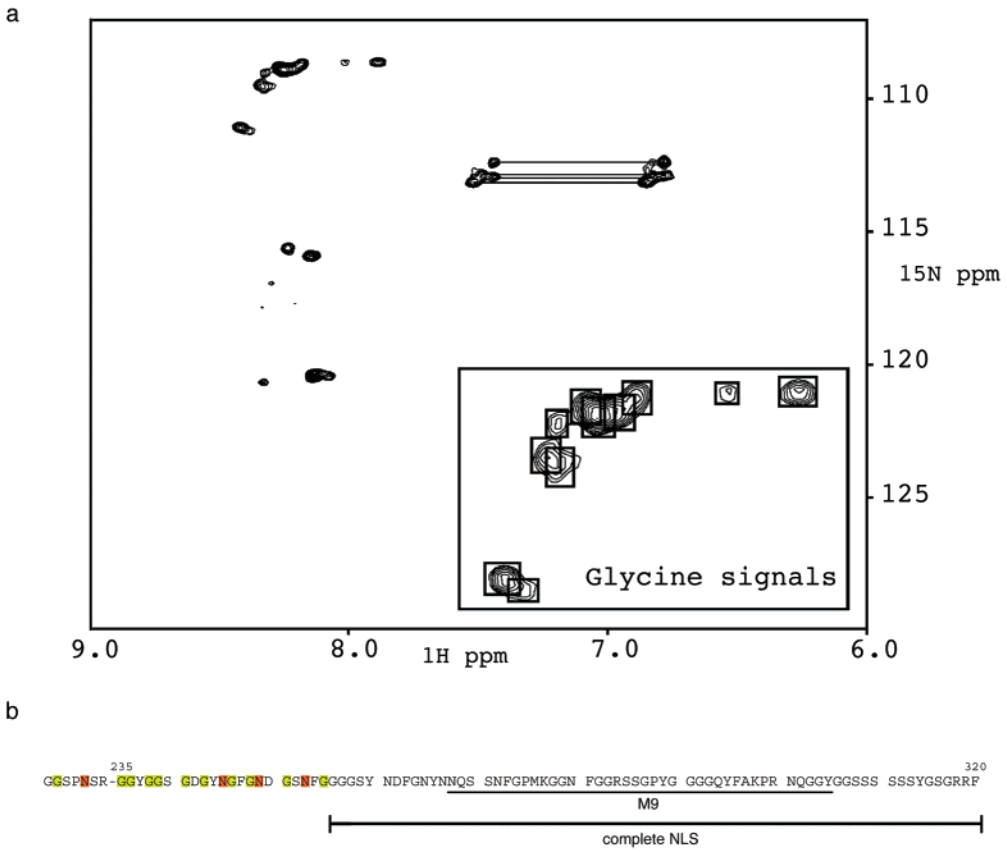


FIGURE 4: (a) $^{1}H/^{15}N$ HSQC spectrum (*13*) of a 1:1 complex of $^{15}N$-labeled M3 peptide and unlabeled Kap$\beta$2. Characteristic side chain amide paired cross-peaks are connected with horizontal lines. The inset shows an expansion of glycine cross-peaks, with individual signals boxed. (b) Sequence of M3 used in NMR experiment. Glycine residues that are disordered are in green, and asparagine residues that are disordered are in orange. The M9 fragment and the new complete NLS, which spans residues 256−320, are both indicated.

the N-terminal 28 residues of M3 do not contact Kap$\beta$2, and that the complete binding epitope consists approximately of the C-terminal 65 residues of the peptide (residues 256−320; Figure 4b).

*Affinities of Kap$\beta$2, cl-Kap$\beta$2, and TL-Kap$\beta$2 for RanGppNHp, Substrates M3, and TAP.* RanGTP binding to Kap$\beta$2 had only been quantitated indirectly through RanGAP inhibition assays (*18*, *19*). We measured direct binding of RanGppNHp to Kap$\beta$2, cl-Kap$\beta$2, and TL-Kap$\beta$2 by fluorescence titration. Ran(mant)GppNHp was titrated with all three Kap$\beta$2 proteins separately, and the decrease in mant fluorescence was fitted to a quadratic equation describing a simple bimolecular association process to obtain the respective affinities (sample binding curves are shown in Figure 5a). All three Kap$\beta$2 proteins bind RanGppNHp with similar, high affinity of 2−5 nM (Table 1). These values are comparable with the $K_D$ of 1 nM obtained from GAP inhibition assay (*18*).

Interactions between Kap$\beta$2 and its substrates have so far not been analyzed quantitatively. We studied the interactions of Kap$\beta$2 with the M3 fragment which contains the NLS of mRNA binding protein A1 (*1*, *2*), and with the NLS of another substrate, mRNA export factor TAP (*4*). We have measured the affinity ($K_D$) of M3 for Kap$\beta$2, cl-Kap$\beta$2, and TL-Kap$\beta$2 by fluorescence titration, and that of the TAP-NLS (TAP residues 61−102) for Kap$\beta$2 and TL-Kap$\beta$2 by surface plasmon resonance. NMR analyses described above indicated that the Kap$\beta$2 binding site on M3 spans residues 256−320 of the substrate (Figure 4b). To measure affinity, residue F247 on MBP-M3a (M3a spans A1 residues 238−320), which is adjacent to the binding site, was replaced with cysteine and labeled with AlexaFluor 350 C2 maleimide, an environment-sensitive fluorophore. MBP-AlexaFluor 350-M3a was titrated with either Kap$\beta$2, cl-Kap$\beta$2, or TL-Kap$\beta$2, and the increase in emitted fluorescence fitted to a quadratic equation describing a simple bimolecular association process to obtain the respective affinities (sample binding curves are shown in Figure 5b). All three Kap$\beta$2 proteins bind substrate M3 with similar, high affinity of 2−3 nM (Table 1).

Sequence analysis of TAP-NLS predicts an absence of secondary structure. This prediction is supported by circular dichroism spectra of TAP-NLS which show no indication of helical or $\beta$-sheet characteristics (data not shown), suggesting that TAP-NLS probably possesses no secondary structure when free in solution. Therefore, immobilization of TAP-NLS to the sensorchip and harsh regeneration conditions should not affect its structure or function. Figure 5c shows binding of Kap $\beta$2 to a TAP-NLS surface at different concentrations of the karyopherin. Kinetic and affinity parameters obtained from SPR analyses are summarized in Table 1. Binding of TAP-NLS to Kap$\beta$2 and TL-Kap$\beta$2 occurs at $k_{on}$ rates in the range of $10^5$ $M^{-1}$ $s^{-1}$, and $k_{off}$ rates are in the range of $10^{-2}$ $s^{-1}$. The resulting $K_D$s for both Kap$\beta$2 proteins binding to TAP-NLS are therefore similar, 18.7 nM for Kap$\beta$2 and 9.0 nM for TL-Kap$\beta$2. Although the affinities for TAP-NLS appear slightly lower, they are still of the same order as interactions with M3.

*Defective Nuclear Import of M3 by TL-Kap$\beta$2.* The ability of RanGppNHp to dissociate import substrate from cl-Kap$\beta$2 and TL-Kap$\beta$2 is severely compromised. We examined the

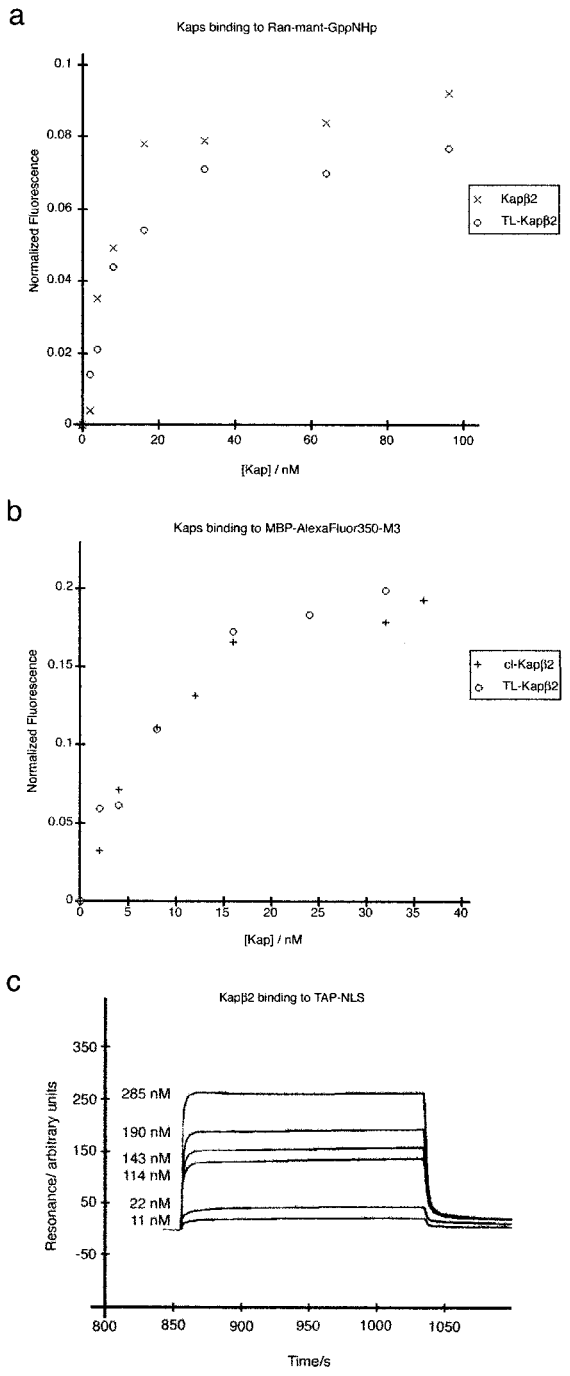


FIGURE 5: Affinity measurements of Kap$\beta$2 proteins binding to substrate and RanGppNHp. (a) Binding curves for titration of Kap$\beta$2 and TL-Kap$\beta$2 into 10 nM Ran(mant)GppNHp. Decrease in fluorescence at 466 nm ($\lambda_{excitation}$ = 350 nm) upon binding was monitored, normalized fluorescence changes are plotted against concentrations of the karyopherins, and the data were fitted to give $K_D$ values. (b) Binding curves for titration of cl-Kap$\beta$2 and TL-Kap$\beta$2 into 15 nM MPB-AF350-M3. Increase in fluorescence at 445 nm ($\lambda_{excitation}$ = 345 nm) upon binding was monitored, normalized fluorescence changes are plotted against concentrations of the karyopherins, and the data were fitted to give $K_D$ values. Normalized fluorescence = (fluorescence − fluorescence$_{initial}$)/(fluorescence$_{maximum}$ − fluorescence$_{initial}$) (c) Kap$\beta$2/TAP-NLS association and dissociation by surface plasmon resonance (SPR). TAP-NLS was immobilized onto a CM5-sensorchip to approximately 400 resonance units. Binding of Kap$\beta$2 to TAP-NLS in a concentration-dependent mode with background response signals subtracted from respective signals obtained from the specific binding reactions for all concentrations of Kap$\beta$2.

Table 1: Affinities of Kap$\beta$2 for Ran·mant-GppNHp and MBP-AlexaFluor350-M3

| Fluorescence Titration[a] | | |
|---|---|---|
| karyopherin | ligand | $K_D$ (nM) |
| Kap$\beta$2 | Ran·mant-GppNHp | 2.1 ± 0.9 |
| cl-Kap$\beta$2 | Ran·mant-GppNHp | 5.0 ± 2.1 |
| TL-Kap$\beta$2 | Ran·mant-GppNHp | 4.2 ± 0.7 |
| Kap$\beta$2 | MBP-AlexaFluor350-M3 | 2.8 ± 0.2 |
| cl-Kap$\beta$2 | MBP-AlexaFluor350-M3 | 2.8 ± 0.5 |
| TL-Kap$\beta$2 | MBP-AlexaFluor350-M3 | 2.4 ± 0.5 |

| SPR Analysis | | | |
|---|---|---|---|
| karyopherin − immobilized ligand | $k_{on}$ ($M^{-1}$ $s^{-1}$) | $k_{off}$ ($s^{-1}$) | $K_D$ (nM) |
| Kap$\beta$2 − TAPNLS | 7.85 × 105 | 1.48 × $10^{-2}$ | 18.7 ± 3.1 |
| TL-Kap$\beta$2 − TAPNLS | 7.1 × 105 | 7.3 × $10^{-3}$ | 9.0 ± 1.1 |

[a] Fluorescence titration experiments were performed in triplicate.

ability of cl-Kap$\beta$2 and TL-Kap$\beta$2 to mediate nuclear import of MBP-M3-GFP, in the presence and absence of Ran. Figure 6a examines the ability of different Kap$\beta$2 proteins to support nuclear accumulation of MBP-M3-GFP in digitonin-permeabilized cells, either with or without Ran. Figure 6b shows the quantitation of nuclear import, obtained under various conditions. Kap$\beta$2 supports nuclear import in the presence of exogenous Ran. In the absence of exogenous Ran, import is significantly decreased, although it is not absent (~25% of import in the presence of exogenous Ran). Similar effects of Ran on Kap$\beta$2 import had been observed previously (*1*, *20*). When similar amounts of TL-Kap$\beta$2 are used, both in the presence and in the absence of exogenous Ran, nuclear import is significantly decreased (~25% of import in the presence of Kap$\beta$2 and Ran). These results indicate that biochemical coupling between Ran and substrate sites is a necessary feature of Kap$\beta$2 function in vivo. Interestingly, the level of nuclear import supported by TL-Kap$\beta$2 is quantitatively similar to that supported by Kap$\beta$2 in the absence of Ran, suggesting that the decrease in nuclear import of Kap$\beta$2 in the absence of Ran is due specifically to loss of Ran-mediated substrate dissociation and not other activities of Ran. Residual nuclear import in the absence of the GTPase may be due to alternative ways of dissociating substrate such as through binding of Kap$\beta$2 to pseudosubstrate sequences on nup98 or nup153 on the nucleoplasmic side of the NPC (*7*, *21*). The inability of TL-Kap$\beta$2 to undergo substrate dissociation in the presence of Ran is reflected in the total loss of Ran-mediated nuclear import.

*TL-Kap$\beta$ Has No Nuclear Export Activity*. TL-Kap$\beta$2 forms a ternary complex with both RanGppNHp and substrate M3, confirming that Ran and substrate sites are spatially distinct yet thermodynamically coupled in native Kap$\beta$2 by the acidic loop. In nuclear import systems, binding of Kap$\beta$ to Ran and substrate is mutually exclusive. In contrast, binding of an export Kap$\beta$ to Ran and substrate is cooperative, and results in formation of a ternary export complex [reviewed in (*5*)]. Thus, the ternary Ran−TL-Kap$\beta$2−substrate complex is reminiscent of a ternary export complex, prompting us to investigate if formation of such a complex is sufficient for export. Digitonin-permeabilized cells were first incubated with MBP-M3-GFP, Kap$\beta$2, and

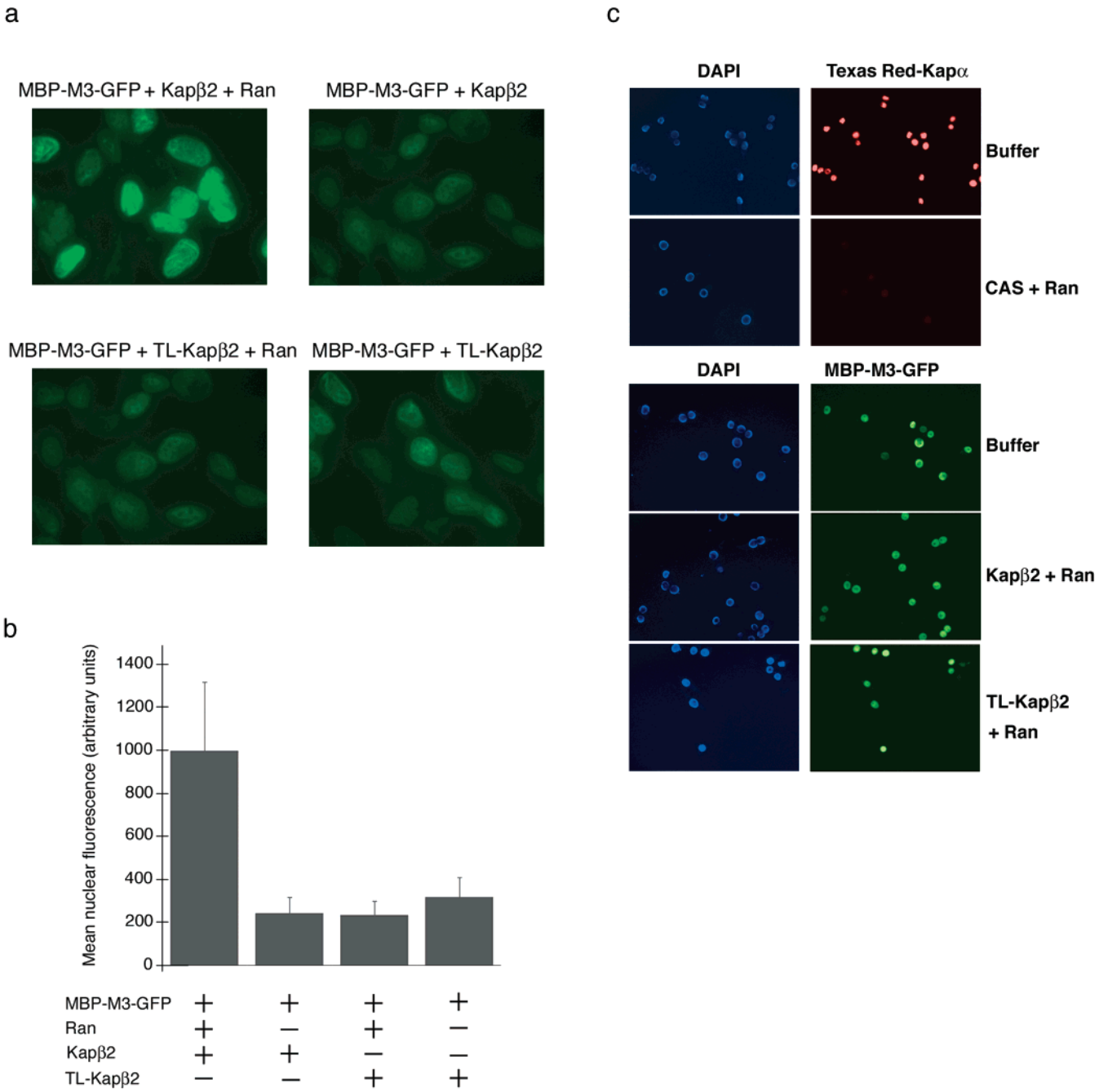


FIGURE 6: Significant decrease in import of M3 by TL-Kap$\beta$2. (a) Import assays were carried out using digitonin-permeabilized HeLa cells that were incubated with 5 $\mu$M MBP-M3-GFP and different import mixes for 20 min at room temperature. Individual import mixtures are indicated. A 2.5 $\mu$M sample of each Kap$\beta$2 and TL-Kap$\beta$2 was used where indicated, Ran refers to a mixture of 2.8 $\mu$M RanGDP, 0.25 $\mu$M RanBP1, 0.175 $\mu$M p10/Ntf2, and 0.4 mM GTP, and the buffer used is TB buffer. Imaging of all samples was identical. (b) Import assays in (a) were quantitated. The mean and standard deviation of more than 70 nuclei are shown for each experiment. (c) Export assays were carried out using digitonin-permeabilized HeLa cells that were subjected to a first incubation to import fluorescent substrate into the nucleus: for control, 0.2 $\mu$M Texas Red-Kap$\alpha$, 0.5 $\mu$M Kap$\beta$1, and Ran mix as in (a); for M3 export, 2 $\mu$M Texas Red-MBP-M3, 5 $\mu$M Kap$\beta$2, and Ran mix. A second incubation with export mix is done after washing. Export mixes are as indicated. 5 $\mu$M each of Kap$\beta$2, TL-Kap$\beta$2, and CAS was used where indicated, Ran refers to the Ran mix described in (a), and the buffer used is TB buffer. Imaging of all samples was identical.

Ran to enable import of fluorescent substrate into the nucleus. A second incubation was done with Kap$\beta$2 or TL-Kap$\beta$2 in the presence of Ran, and the resultant nuclear fluorescence was examined. A control experiment with Texas Red-Kap$\alpha$, Kap$\beta$1, and Ran to import fluorescent Kap$\alpha$ into the nucleus followed by an incubation of export karyopherin CAS and Ran clearly shows export of fluorescent Kap$\alpha$ from the nucleus (*22*, *23*). Figure 6c shows the results of these export assays. Addition of TL-Kap$\beta$2 as a possible export factor did not change the nuclear fluorescence of substrate MBP-M3-GFP when compared to addition of Kap$\beta$2 or buffer. These results indicate that TL-Kap$\beta$2 is not able to export M3 even though it forms a ternary assembly that resembles an export complex.

## DISCUSSION

The structure of the Kap$\beta$2−RanGppNHp complex suggested that the acidic loop of Kap$\beta$2 is important in coupling

the Ran and substrate binding sites of the karyopherin to mediate substrate dissociation in the presence of the GTPase (*10*). Using Kap$\beta$2 proteins with modified acidic loops, we have now demonstrated that the Kap$\beta$2 acidic loop is crucial for Ran-mediated substrate dissociation, as it provides a physical conduit between the spatially distinct substrate and Ran sites. The disruption of Ran-mediated substrate dissociation in these modified Kap$\beta$2s translates to a large decrease in nuclear import activity. We have determined that approximately 75% of Kap$\beta$2 nuclear import is Ran-mediated, which is abolished when the acidic loop is disrupted. This is the first demonstration that Ran-mediated substrate dissociation of Kap$\beta$2 and not merely other Ran activities defines the Kap$\beta$2 Ran-dependent nuclear import. These results also support previous findings that other means of substrate dissociation independent of Ran play important roles in nuclear import.

The central feature of the proposed Ran-mediated substrate dissociation mechanism for Kap$\beta$2 involved its 62-residue acidic loop which interacts with both Ran and the substrate binding site of Kap$\beta$2 (*10*). When Kap$\beta$2 binds RanGppNHp, distal portions of its acidic loop occupy a site similar to or overlapping with the substrate binding site, thus displacing substrate from Kap$\beta$2 and releasing it into the nucleus. To determine the contribution of the acidic loop of Kap$\beta$2 to Ran-mediated substrate dissociation, we have generated two Kap$\beta$2 proteins with modified acidic loops. Fortuitously, thrombin cleaves in the middle of the loop between residues 338 and 339 to generate cl-Kap$\beta$2 with a disconnected acidic loop. The overall structure of this protein appears to be similar to that of wild-type Kap$\beta$2 with similar functional activities such as bimolecular Ran binding and substrate binding, and similar hydrodynamic behavior. However, cl-Kap$\beta$2 fails to dissociate from substrate in the presence of RanGppNHp. Since the only feature of Kap$\beta$2 that was altered is the severed acidic loop, these results indicate the acidic loop is critical for coupling Ran and substrate binding sites to allow Ran-mediated substrate dissociation.

The second modified Kap$\beta$2 is the recombinant TL-Kap$\beta$2 mutant, where the acidic loop was truncated by substitution of residues 340−362 with a 7-residue glycine and serine linker. Residues 340−362 mediate all the contacts between the acidic loop and the C-terminal arch of Kap$\beta$2 in the Ran complex (*10*). None of the loop residues that contact Ran were removed in this mutant. Like cl-Kap$\beta$2, TL-Kap$\beta$2 is similar to wild-type Kap$\beta$2 in terms of bimolecular Ran binding, substrate binding, and hydrodynamic properties. Like cl-Kap$\beta$2, TL-Kap$\beta$2 is defective in substrate dissociation in the presence of RanGppNHp. Furthermore, TL-Kap$\beta$2 can form a ternary complex, with both Ran and substrate binding simultaneously. Again, like cl-Kap$\beta$2, defective Ran-mediated substrate dissociation indicates that a complete acidic loop, especially the distal portions missing in TL-Kap$\beta$2, is essential for transmission of signal from Ran to substrate site to effect substrate dissociation. In addition, the ability of TL-Kap$\beta$2 to bind substrate and Ran simultaneously suggests that binding sites for the two Kap$\beta$2 ligands are indeed spatially distinct.

Although qualitative binding assays show Kap$\beta$2, cl-Kap$\beta$2, and TL-Kap$\beta$2 all bind both M3 and Ran with high affinity, rigorous description of the mechanism of action of the modified Kap$\beta$2s and the mechanism of Ran-mediated substrate dissociation requires quantitation of binding affinities. We titrated each Kap$\beta$2, cl-Kap$\beta$2, and TL-Kap$\beta$2 into fluorescent Ran(mant)GppNHp, and measurements of fluorescence quenching gave affinities of 2.1, 5.0, and 4.2 nM for the respective Kap−Ran interactions. There are no significant differences in affinities between Kap$\beta$2 and the modified Kap$\beta$2s, and the measured $K_D$s are similar to the 1 nM affinity for Kap$\beta$2 binding to RanGTP determined indirectly through inhibition assays (*18*). These results indicate that neither cleavage of the acidic loop in cl-Kap$\beta$2 nor loop truncation in TL-Kap$\beta$2 have affected the affinity of their interactions with RanGppNHp. Therefore, the observed loss of Ran-mediated substrate dissociation in both cases cannot be attributed to decreased affinity of the Kap$\beta$2 proteins for Ran.

Titration of each Kap$\beta$2, cl-Kap$\beta$2, and TL-Kap$\beta$2 into fluorescent MBP-M3 gave measured affinities of 2.8, 2.4, and 2.8 nM, respectively. Affinities of Kap$\beta$2 and TL-Kap$\beta$2 for another substrate, TAP-NLS, were determined by SPR analysis to be 18.7 and 9.0 nM, respectively. All three Kap$\beta$2 proteins have similar high affinities for substrates, corresponding to values determined for Kap$\alpha$ binding to the classical basic-NLS (10 nM) by fluorescence anisotropy (*24*). Modification of the acidic loop in cl-Kap$\beta$2 and TL-Kap$\beta$2 has not changed the affinity for substrate. More importantly, neither cleavage of the loop nor removal of portions capable of interacting with the C-terminal arch, where substrate is also proposed to bind, has resulted in increased affinity for substrate, which could prevent dissociation by Ran. Since neither binary Ran binding nor substrate binding has been affected by modification of the acidic loop, the loss of Ran-mediated substrate dissociation must be due to the inability of the modified loops to couple, and transmit information between the two ligand binding sites.

We refer to the mechanism of Ran-mediated substrate dissociation in Kap$\beta$2 as a negative allosteric mechanism. Allosteric effect is a mechanistic term that sometimes causes confusion, especially when it is equated with cooperativity exhibited by classical oligomeric allosteric enzymes (*25*). 'Allosteric' as used in this paper refers to the term's original definition. In Greek, *allos* is other, and *stereos* is rigid, solid, or space (*26*). An allosteric effect refers to indirect interactions between distinct specific binding sites (*27*, *28*). Thus, the term allosteric effect appropriately describes Ran-mediated substrate dissociation in Kap$\beta$2: the acidic loop mediates indirect interactions between the distinct Ran site in the N-terminal arch and the substrate site in the C-terminal arch of Kap$\beta$2. Ran thus acts as a negative heterotropic effector of Kap$\beta$2; its binding decreases the affinity of Kap$\beta$2 for substrate. Although classical allostery is often equated with cooperativity exhibited by oligomeric enzymes, it has long been recognized that a heterotropic effect is possible in monomeric proteins that contain two or more distinct binding sites. But obviously, homotropic effects, which are one of the defining characteristics of allosteric enzymes, are possible only in oligomeric proteins (*28*).

The similar high affinities of Kap$\beta$2, cl-Kap$\beta$2, and TL-Kap$\beta$2 for the NLS of substrates A1 and TAP imply that the acidic loop does not participate in substrate binding. We have observed that both isolated Kap$\beta$2 and the Kap$\beta$2−M3 complex are sensitive to proteolysis at the acidic loop by a variety of proteases, while the Kap$\beta$2−RanGppNHp

complex remains protected (Figure 3 of the Supporting Information). These observations suggest that the acidic loop participates in binding of Ran but not substrate. We predict that the acidic loop is disordered and mobile in both the free and substrate-bound states, but upon binding Ran becomes significantly structured through interactions with Ran and the C-terminal arch of Kap$\beta$2. Interestingly, the acidic loops of Kap$\beta$1 and Kap$\beta$2 function differently. In Kap$\beta$1, the acidic loop is only 11 residues long, and binds both substrate Kap$\alpha$ and RanGppNHp in the respective binary complexes (*14*, *15*). Kap$\beta$1 acidic loop residues D340 and W342 as well as residues E281 and D288 in HEAT repeat 7 contact both RanGppNHp and Kap$\alpha$. Thus, binding of Ran and Kap$\alpha$ to Kap$\beta$1 is isosteric, with common or overlapping binding sites, in contrast to allosteric interactions of the equivalent ligands to Kap$\beta$2 in distinct sites. Structures of Kap$\beta$1 and Kap$\beta$2 are similar, with Ran binding to the N-terminal and substrate binding to the C-terminal HEAT repeats. Both karyopherins have central acidic loops. But, substrate dissociation appears to be accomplished through fundamentally different mechanisms. Structural analyses of the Kap$\beta$1−Kap$\alpha_{11-54}$ and Kap$\beta1_{1-462}$−RanGppNHp complexes indicate that large conformational changes involving rearrangements of Kap$\beta$1 HEAT repeats likely accompany the transition from a Kap$\beta$1−substrate complex to a Kap$\beta$1−Ran complex (*14*, *15*). Based on these structural observations, Ran-mediated substrate dissociation in Kap$\beta$1 probably occurs through a combination of binding site competition and GTPase-induced conformational changes in the karyopherin (*5*). It is currently unclear if HEAT repeat rearrangements accompany ligand binding in Kap$\beta$2. The flexible segmental nature of Kap$\beta$ HEAT repeats may allow accumulation and propagation of structural changes from the individual units to generate a large repertoire of binding surfaces and mode of regulation of ligand binding activities. Structures of unliganded Kap$\beta$2 and a Kap$\beta$2−substrate complex will provide insights into the range of possible conformational states for Kap$\beta$2. Potential acidic loops in the central region of other Kap$\beta$s have also been observed. Kap$\beta$3, Kap123p, Kap108p/Sxm1p, Kap109p/CAS/Cse1p, Kap127p/Los1p/exportin-t, Exportin4, Exportin5, RanBP7, and RanBP8 all seem to contain a stretch of acidic residues that could be part of a central loop. It will be interesting to learn if these acidic sequences function differently in import versus export.

A single round of nuclear import can be divided into four key steps: substrate recognition, targeting of the import complex to the NPC, translocation through the NPC, and substrate dissociation in the nucleus. Our biochemical data suggest that TL-Kap$\beta$2 likely shares the same activity as wild-type Kap$\beta$2 in the first three steps of substrate recognition, NPC targeting, and translocation. We have successfully uncoupled Ran binding from substrate dissociation in TL-Kap$\beta$2, and this system provides an opportunity to assess the contribution of Ran-mediated substrate dissociation to total nuclear import by Kap$\beta$2. We used digitonin-permeabilized HeLa cells to monitor nuclear import by Kap$\beta$2, cl-Kap$\beta$2, and TL-Kap$\beta$2, both in the presence and in the absence of Ran and GTP. As previously reported (*1*, *2*, *20*), we also observe a significant decrease in Kap$\beta$2 nuclear import in the absence of exogenous Ran. Quantitation of nuclear fluorescence suggests that approximately 75% of nuclear import was lost when no Ran is added. Nuclear import with TL-Kap$\beta$2 was reduced to a similar low level both in the presence and in the absence of exogenous Ran and nucleotide. In the experiment with TL-Kap$\beta$2 and Ran, the only Ran activity that is missing is the Kap$\beta$2−substrate dissociation activity. These data thus suggest that approximately 75% of Kap$\beta$2-mediated import is Ran-dependent, and this import is defined entirely by Ran-mediated substrate dissociation and not any other activity of Ran. Residual import is observed both in the absence of Ran and with TL-Kap$\beta$2. This residual Kap$\beta$2 import indicates completion of import via alternative means of substrate dissociation (*7*−*9*). In this regard, Nakielny et al. and Fontoura et al. identified M9-like sequences in the NPC components, Nup153 and Nup98, respectively (*7*, *21*). Both nucleoporins have been localized to the NPC and the interior of the nucleus, which could be convenient locations for substrate dissociation. Nup98 has been shown to compete with substrate fragment M3 for Kap$\beta$2, suggesting that the M9-like sequences in Nup98 and Nup153 could act as pseudosubstrates to dissociate substrate from Kap$\beta$2 upon reaching the nucleoplasmic side of the NPC (*7*). RanGTP could then dissociate Kap$\beta$2 from the nucleoporin pseudosubstrate site to be recycled to the cytoplasm.

In nuclear import, binding of Kap$\beta$s to RanGTP and substrates is mutually exclusive. In contrast, interactions between export Kap$\beta$s, RanGTP, and export substrates seem to be cooperative and result in the formation of a ternary export complex (*5*). The interactions of TL-Kap$\beta$2 with Ran and substrates no longer resemble that of an import factor. The Kap$\beta$2 mutant binds substrate and Ran simultaneously to form a ternary assembly that is analogous to an export complex. Export assays monitoring the nuclear fluorescence of M3 show that TL-Kap$\beta$2 does not export its substrate. These results emphasize that formation of a ternary complex containing Kap$\beta$, substrate, and RanGTP, while necessary (*22*, *29*), is not sufficient for export. Such a ternary complex recognizes substrate in the nucleus, may target substrate to the NPC, and may even be translocation-competent toward the cytoplasm. However, the ternary complex is unable to undergo the last and crucial step of substrate dissociation. TL-Kap$\beta$2 binds substrate regardless of the nucleotide state of Ran. Nucleotide hydrolysis catalyzed by RanGAP on the cytoplasmic side of the NPC or interactions with RanBP1 will decrease Ran−TL-Kap$\beta$2 interactions. However, since Ran and substrate dissociation are uncoupled in TL-Kap$\beta$2, and there is no positive or negative cooperativity between the ligands, TL-Kap$\beta$2−substrate interactions remain unaffected, and substrate is not released into the cytoplasm. We have removed the negative heterotropic effect of Ran on substrate binding in TL-Kap$\beta$2. To convert an import Kap$\beta$ to an export factor, one would also need to engineer in a positive heterotropic effect or cooperativity where Ran binding increases the affinity of substrate, such that removal of Ran decreases the affinity of substrate to allow dissociation into the cytoplasm. Such protein engineering requires understanding of the basis of cooperativity in nuclear export complex formation.

## ACKNOWLEDGMENT

We thank Mike Seidman for preliminary work on fluorescence titration, Neris Bonifaci for the M3 expression

construct, Nabeel Yaseen for the Kap$\beta$1 expression construct, Jing-dong Han for the CAS expression construct, Ken Marians for the use of the BIAcore facility, Joe Fernandez of the Rockefeller University Protein DNA Technology Center for protein N-terminal sequencing, Tom Sakmar for use of the fluorescence spectrophotometer, Eduardo Torres, Matthias Buck, Susana Chaves, Gopala Aradhyam, and Elias Coutaves for technical instructions, and Stepanka Cermanova for technical support.

## SUPPORTING INFORMATION AVAILABLE

Three figures showing gel filtration elution profiles, CD spectra, and proteolysis of Kap$\beta$2. This material is available free of charge via the Internet at http://pubs.acs.org.

## REFERENCES

1. Bonifaci, N., Moroianu, J., Radu, A., and Blobel, G. (1997) *Proc. Natl. Acad. Sci. U.S.A. 94*, 5055−5060.
2. Pollard, V. W., Michael, W. M., Nakielny, S., Siomi, M. C., Wang, F., and Dreyfuss, G. (1996) *Cell 86*, 985−994.
3. Siomi, M. C., Eder, P. S., Kataoka, N., Wan, L., Liu, Q., and Dreyfuss, G. (1997) *J. Cell Biol. 138*, 1181−1192.
4. Truant, R., Kang, Y., and Cullen, B. R. (1999) *J. Biol. Chem. 274*, 32167−32171.
5. Chook, Y. M., and Blobel, G. (2001) *Curr. Opin. Struct. Biol. 11* (6), 703−715.
6. Yoshida, K., and Blobel, G. (2001) *J. Cell Biol. 152*, 729−740.
7. Fontoura, B. M., Blobel, G., and Yaseen, N. R. (2000) *J. Biol. Chem. 275*, 31289−31296.
8. Pemberton, L. F., Rosenblum, J. S., and Blobel, G. (1999) *J. Cell Biol. 145*, 1407−1417.
9. Lee, D. C., and Aitchison, J. D. (1999) *J. Biol. Chem. 274*, 29031−29037.
10. Chook, Y., and Blobel, G. (1999) *Nature 399*, 230−237.
11. Fridell, R. A., Truant, R., Thorne, L., Benson, R. E., and Cullen, B. R. (1997) *J. Cell Sci. 110*, 1325−1331.
12. Siomi, H., and Dreyfuss, G. (1995) *J. Cell Biol. 129*, 551−560.
13. Kay, L. E., Keifer, P., and Saarinen, T. (1992) *J. Am. Chem. Soc. 114*, 10663−10665.
14. Cingolani, G., Petosa, C., Weis, K., and Muller, C. W. (1999) *Nature 399*, 221−229.
15. Vetter, I. R., Arndt, A., Kutay, U., Gorlich, D., and Wittinghofer, A. (1999) *Cell 97*, 635−646.
16. Yaseen, N. R., and Blobel, G. (1997) *Proc. Natl. Acad. Sci. U.S.A. 94*, 4451−4456.
17. Cavanagh, J., Frairbrother, W. J., Palmer, A. G., and Skelton, N. J. (1996) *Protein NMR Spectroscopy principle and Practice*, Academic Press, San Diego.
18. Gorlich, D., Pante, N., Kutay, U., Aebi, U., and Bischoff, F. R. (1996) *EMBO J. 15*, 5584−5594.
19. Floer, M., and Blobel, G. (1996) *J. Biol. Chem. 271*, 5313−5316.
20. Ribbeck, K., Kutay, U., Paraskeva, E., and Gorlich, D. (1999) *Curr. Biol. 9*, 47−50.
21. Nakielny, S., Shaikh, S., Burke, B., and Dreyfuss, G. (1999) *EMBO J. 18*, 1982−1995.
22. Kutay, U., Bischoff, F. R., Kostka, S., Kraft, R., and Gorlich, D. (1997) *Cell 90*, 1061−1071.
23. Moroianu, J., Blobel, G., and Radu, A. (1997) *Proc. Natl. Acad. Sci. U.S.A. 94*, 9699−9704.
24. Hodel, M. R., Corbett, A. H., and Hodel, A. E. (2001) *J. Biol. Chem. 276*, 1317−1325.
25. Ricard, J., and Cornish-Bowden, A. (1987) *Eur. J. Biochem. 166*, 255−272.
26. Helmstaedt, K., Krappman, S., and Braus, G. H. (2001) *Microbiol. Mol. Biol. Rev. 65*, 404−421.
27. Monod, J., Changeux, J.-P., and Jacob, F. (1963) *J. Mol. Biol. 6*, 306−329.
28. Monod, J., Wyman, J., and Changeux, J.-P. (1965) *J. Mol. Biol. 12*, 88−118.
29. Fornerod, M., Ohno, M., Yoshida, M., and Mattaj, I. W. (1997) *Cell 90*, 1051−1060.
30. Nicholls, A., Sharp, K. A., and Honig, B. (1991) *Proteins: Struct., Funct., Genet. 11*, 281−296.

BI012122P